THE JOURNAL OF PHYSICAL CHEMISTRY LETTERS
A JOURNAL OF THE AMERICAN CHEMICAL SOCIETY



pubs.acs.org/JPCL
Letter

# Polariton Control of Molecular Charge Transfer in Perylene Diimide Semiconductors

Rao Fei, Victoria Quirós-Cordero, Demelza Wright, Debjit Ghoshal, Justin C. Johnson, Ivan I. Smalyukh, Carlos Silva-Acuña, Natalie Stingelin, and Jao van de Lagemaat*

Cite This: J. Phys. Chem. Lett. 2026, 17, 790−796
Read Online



**ABSTRACT:** We report the modulation of molecular charge transfer in a bay-substituted perylene diimide derivative embedded in a planar distributed Bragg reflector microcavity. Angle-resolved reflectance spectra confirm the formation of upper and lower polaritons with clear Rabi splitting, indicating strong coupling between the cavity mode and molecular excitons. Using broadband transient absorption spectroscopy, we compare the ultrafast dynamics of cavity and non-cavity films. While excited-state absorption and stimulated emission pathways remain largely unchanged, kinetic modeling reveals a moderate increase in the charge transfer rate and yield under strong coupling. This enhancement is attributed to a reduction in the effective driving force via the formation of the lower polariton, placing the system deeper into the Marcus inverted regime. Our results demonstrate a promising non-chemical method leveraging cavity quantum electrodynamics to modulate charge separation processes in molecular semiconductors.

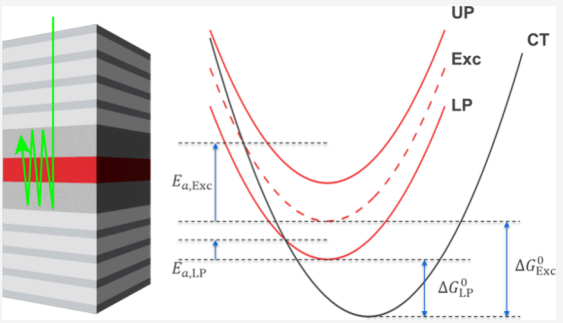




Strong light−matter coupling emerges when the interaction between a material excitation and a confined electromagnetic mode becomes coherent and reversible on time scales faster than their respective losses.[1,2] In this regime, the system evolves into new eigenstates called upper and lower polaritons, which inherit characteristics from both light and matter constituents.[3] The energy separation between these polariton branches, known as the Rabi splitting, reflects the strength of the coupling and depends on both oscillator strength and mode confinement.[4] Because the polariton states are part light and part matter, their properties, including energy dispersion, decay rates, and transition pathways, can be tuned by modifying the cavity environment without altering the chemical identity of the material.[5−7] This makes strong coupling a powerful tool to modulate excited-state behavior and energy flow in molecular systems, which can lead to not only enhanced charge separation in optoelectronic devices, such as organic solar cells, but also dynamic control of such devices by external stimuli, potentially enabling photonic switches, reservoir computers, quantum devices, and more.[8]

Recent studies have demonstrated that strong light−matter coupling can reshape excited-state dynamics by modulating ultrafast relaxation pathways and suppressing non-radiative losses. In particular, polaritonic systems have been shown to alter exciton interactions and redistribute energy flow within the coupled exciton−photon manifold, offering new routes to control nonlinear optical behavior and emission characteristics.[7,9] Polaritons have also been harnessed to enable long-range energy transfer,[10] manipulate triplet dynamics and delayed fluorescence,[11,12] steer photoisomerization pathways,[13] and enhance charge separation in donor−acceptor systems.[14] These demonstrations underscore the versatility and potential of cavity-enhanced interactions for tailoring fundamental photophysical and photochemical processes. While these effects are often attributed to polaritons, it is increasingly recognized that dark states, which are the non-emissive excitonic modes arising from strong coupling, may also play supporting roles in relaxation and transport.[15−18] Recently, it was theoretically shown that the presence of dark states can drive the polariton-mediated electron transfer rates up by orders of magnitude even in the presence of disorder and in lossy cavities.[19]

Perylene diimide (PDI) derivatives are well-studied organic chromophores valued for their high photostability, strong absorption, and tunable electronic structure.[20,21] The propensity to form excimers and charge-transfer (CT) states through $\pi-\pi$ interactions also makes them sensitive probes of photophysical processes.[22,23] To reduce aggregation and suppress intermolecular interactions, structural modifications, such as large bay substitutions, are often introduced.[24] In such

Received: August 18, 2025
Revised: December 12, 2025
Accepted: December 17, 2025
Published: January 7, 2026

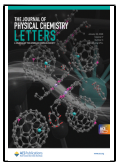

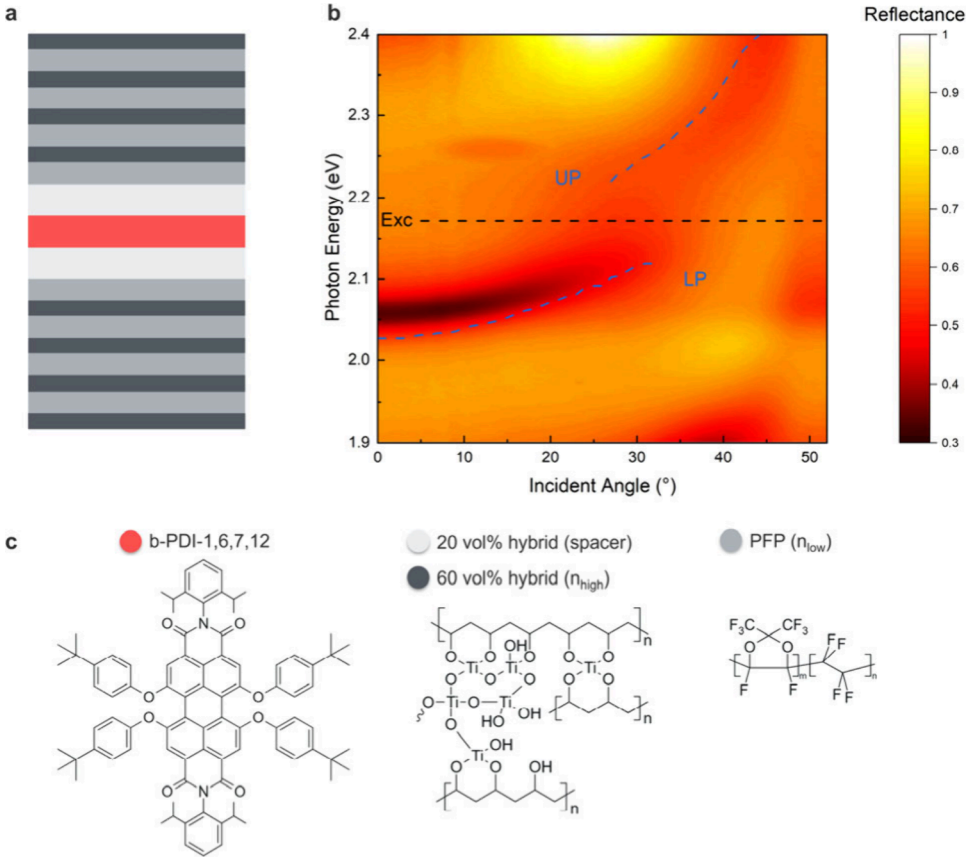


**Figure 1.** Strong light−matter coupling in a DBR cavity system. (a) Microcavity architecture. (b) Angular reflectance dispersion of the system, with UP and LP peak positions predicted with simulation (blue dashed lines) and the polariton bands exhibiting an anticrossing behavior at the exciton energy (black dash line). (c) Chemical structures of the materials used for cavity fabrication: b-PDI-1,6,7,12, a high-refractive index inorganic/organic hybrid (described in refs 26 and 29−31), and the low-refractive index PFP (refs 26, 29, and 30). For the hybrid material, the volume fraction of the titanium oxide hydrate content in poly(vinyl alcohol) is given, which enables fine control of the material refractive index (for more details, see the Cavity Fabrication section in the Supporting Information).[26,29−31]

systems, CT is generally suppressed unless symmetry is broken, either through molecular asymmetry or external perturbation.[25]

In this work, we investigate the effects of strong light−matter coupling on the excited-state dynamics of b-PDI-1,6,7,12, a bay-substituted PDI derivative. By embedding the PDI film in a planar distributed Bragg reflector (DBR) microcavity, we observe clear Rabi splitting and polariton dispersion, confirming the formation of exciton−polaritons. Using broadband ultrafast transient absorption spectroscopy, which tracks how excited states evolve over time, we compare the photodynamics of cavity and non-cavity samples and find that cavity coupling moderately enhances the rate of intramolecular CT while leaving other processes largely unchanged. This demonstrates that, in systems designed to limit intermolecular interactions, strong coupling can reshape internal excited-state pathways and enhance the charge transfer, providing a new approach to modulating charge separation and relaxation in molecular semiconductors.

*Strong Light−Matter Coupling in a Microcavity System*. Figure 1 shows the light−matter strong coupling in the microcavity system. The microcavity is fabricated based on two four-bilayer DBRs as mirrors,[26] including b-PDI-1,6,7,12 as the active semiconductor within the spacer.

The DBR cavity exhibits a broad high-reflectivity stopband, within which two distinct reflection dips appear. This splitting of PDI's exciton peak, along with the angular-dependent dispersion of these features (also see Figure S1b of the Supporting Information), demonstrates strong light−matter coupling, as further supported by electromagnetic simulations based on the finite-difference method (blue dashed lines in Figure 1b; also see Figure S1c of the Supporting Information). The Rabi splitting, defined as the minimum energy separation between the upper polariton (UP) and lower polariton (LP) bands, is found to be $\Omega_R$ = 120 meV at 29°, a value well above $k_BT$ and larger than the average of the exciton line width (145 meV) and the empty cavity mode (66 meV); therefore, the system is in the strong coupling regime and is typical for organic semiconductors coupled in low-$Q$ cavities.[27,28] We do not observe strong coupling at the second (0−1) excitonic transition at 2.31 eV, which is likely due to this transition having a much larger line width than the first excitonic transition, and it therefore cannot reach strong coupling.

Large bay substitutions in PDI derivatives are known to increase the intermolecular distance and reduce the tendency to aggregate.[26] As shown in Figure 2a, the steady-state absorption and photoluminescence (PL) spectra of the PDI film closely follow those in the solution, indicating a monomeric state with no significant aggregation. The exciton peak (0−0 transition) at 2.17 eV has higher intensity than its vibronic satellite (0−1 transition, 2.33 eV), suggesting less $\pi$-stacking than common H-aggregates for the PDI derivatives.[32]


https://doi.org/10.1021/acs.jpclett.5c02566
J. Phys. Chem. Lett. 2026, 17, 790−796

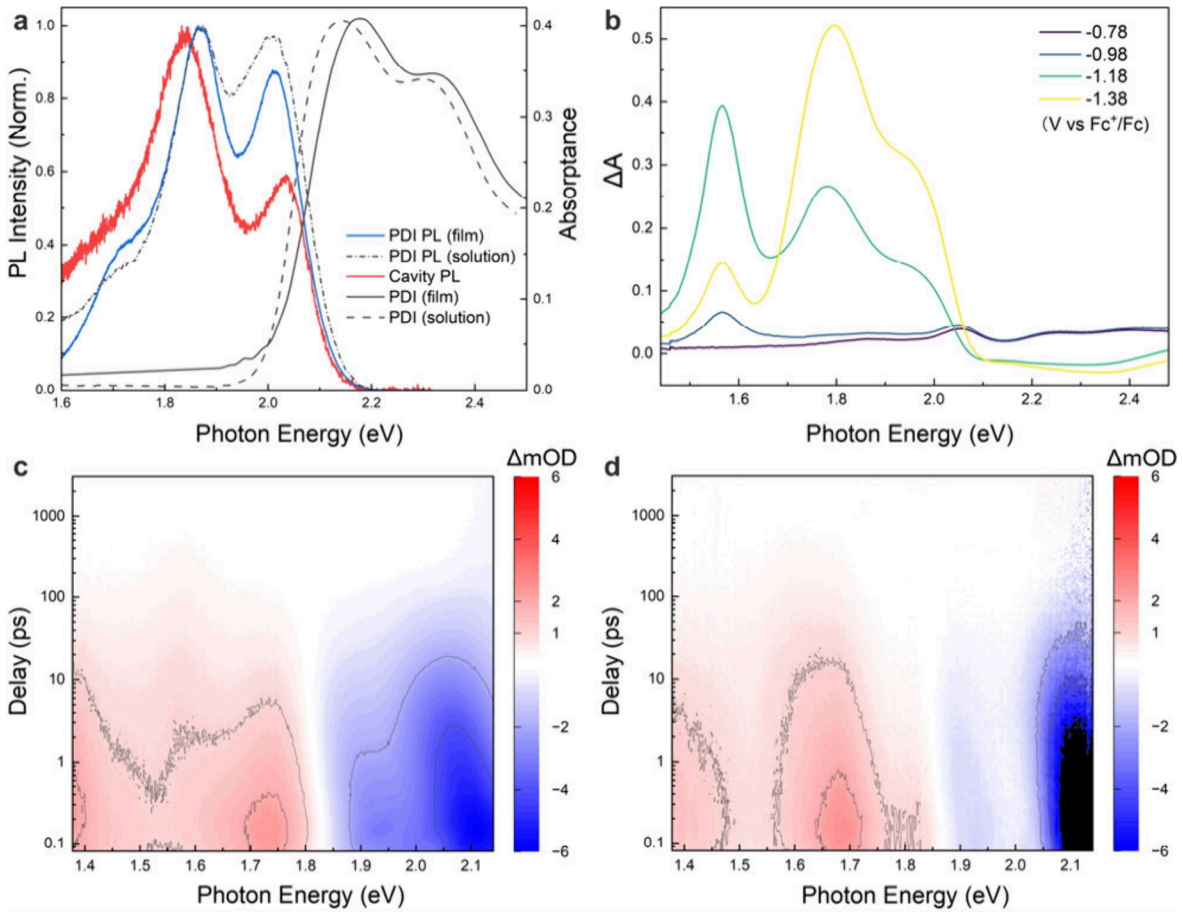


**Figure 2.** Spectroscopy characterizations of b-PDI-1,6,7,12 and cavity sample. (a) UV−vis absorption and PL spectra with 2.33 eV excitation. The solution absorptance is taken from 0.25 mM b-PDI-1,6,7,12 in acetonitrile solution and normalized to that of the film. The solution PL is measured from a 0.025 mM solution. (b) Electrochemical spectroscopy of reduced b-PDI-1,6,7,12. Each spectrum is plotted as the difference from the open-circuit potential spectrum. TA spectra for (c) b-PDI-1,6,7,12 and the (d) cavity sample are measured with excitation at an exciton energy of 2.17 eV and a fluence of 1.93 mJ/cm$^2$.

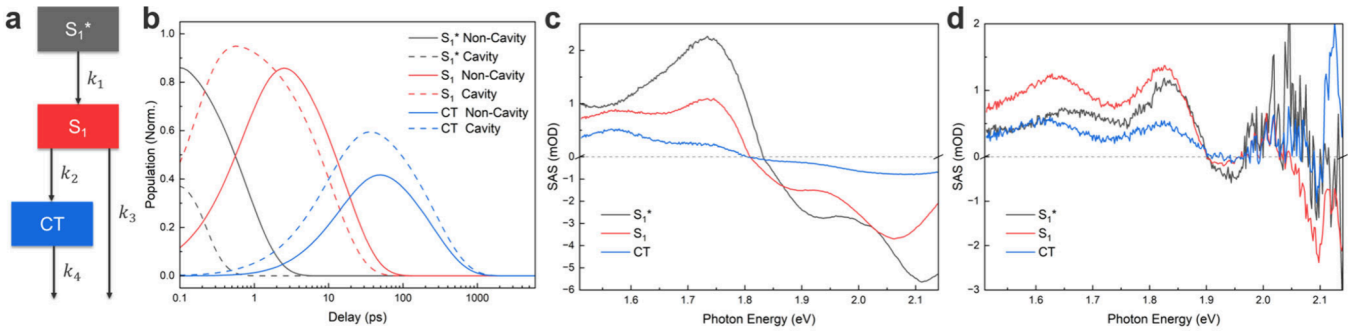


**Figure 3.** Target analysis of the PDI and cavity samples. (a) Schematic of the spectral sequence fitted as the kinetic model. (b) Population dynamics of sequential evolution. Species associated spectra of the (c) non-cavity sample excited at 2.17 eV (exc) and the (d) cavity sample excited at 2.12 eV (LP). Note the scale differences between positive and negative y-axis directions in c and d.

On the other hand, the PL spectrum in the cavity features suppressed intensities from 0 to 0 compared to the 0−1 transition, which may indicate cavity-modified radiative decay channels or the cavity acting as an optical filter according to the stop-band profile (Figure S1d of the Supporting Information).[33] While the altered PL profile could include contributions from LP emission, such an assignment is not made definitively due to the complexity of polaritonic emission pathways.[34]

*Molecular CT Dynamics.* Figure 2c shows the room temperature broadband transient absorption spectrum for the non-cavity sample pumped at the exciton energy of b-PDI-1,6,7,12 (2.17 eV). Distinct ground-state bleach (GSB) overlapping with red-shifting stimulated emission (SE) can be observed above 1.85 eV, following the steady-state absorption and photoluminescence spectra (Figure 2a). The peak at 1.73 eV corresponds to a singlet excited-state absorption (ESA), consistent with the behavior observed in many PDI derivatives.[32,35,36] The low-intensity peak at 1.57 eV



https://doi.org/10.1021/acs.jpclett.5c02566
J. Phys. Chem. Lett. 2026, 17, 790−796

Table 1. Fitted Rate Constants from Target Analysis Measured at the Same Fluence of 3.11 mJ/cm$^2$

| sample (excitation) | b-PDI-1,6,7,12 (ps$^{-1}$) (exc) | cavity (ps$^{-1}$) (UP) | cavity (ps$^{-1}$) (exc) | cavity (ps$^{-1}$) (LP) |
|---|---|---|---|---|
| $k_1$ | 1.267 ± 0.041 | 1.028 ± 0.057 | 1.727 ± 0.114 | 8.632 ± 1.767 |
| $k_2$ | 0.0305 ± 0.0029 | 0.0442 ± 0.0040 | 0.0515 ± 0.0095 | 0.0628 ± 0.0043 |
| $k_3$ | 0.0301 ± 0.0028 | 0.0600 ± 0.0040 | 0.0299 ± 0.0085 | 0.0295 ± 0.0042 |
| $k_4$ | 0.0039 ± 0.0002 | 0.0036 ± 0.0004 | 0.0045 ± 0.0005 | 0.0037 ± 0.0002 |
| $k_2/(k_2 + k_3)$ | 0.503 ± 0.033 | 0.424 ± 0.027 | 0.633 ± 0.079 | 0.680 ± 0.034 |

characterized by a long lifetime is assigned to the CT state, which is supported by electrochemical spectroscopy measurements (Figure 2b), where the radical anion shows a spectral peak at 1.57 eV and the dianion has an absorption peak at 1.78 eV (Figure S2 of the Supporting Information). No significant change in TA spectra is observed under air-free conditions, ruling out oxygen-sensitive triplet states. The TA spectrum for the cavity (Figure 2d) is measured with the same excitation energy and fluence. The cavity shows clear enhancement on GSB and exhibits slight shifting for all the features, which is due to the cavity modification of the steady-state and excited-state spectra[37] and the dynamics of the coupled exciton.[7]

An overall kinetic model encompassing both ESA and CT states is proposed as in Figure 3a, informed by singular value decomposition, which indicates that three spectral components sufficiently describe the data set. Representative traces among the spectral range are fitted to the differential equations 1−4 using the corresponding kinetic model

$$P(t) = \frac{1}{\sqrt{2\pi}\sigma} \exp\left(-\frac{(t - t_0)^2}{2\sigma^2}\right) \quad (1)$$

$$\frac{dy_0}{dt} = P(t)N - k_1 y_0 \quad (2)$$

$$\frac{dy_1}{dt} = k_1 y_0 - (k_2 + k_3) y_1 \quad (3)$$

$$\frac{dy_2}{dt} = k_2 y_1 - k_4 y_2 \quad (4)$$

where $P(t)$ is the normalized Gaussian pump pulse centered at $t_0$ with width $\sigma$, $N$ is the initial population amplitude, which acts as a scaling parameter and is not essential to the core dynamics, and $k_i$ values are first-order rate constants corresponding to the decay channels.

The cavity sample is excited at three different energies, the UP at 2.19 eV, the exciton at 2.17 eV, and the LP at 2.12 eV, respectively, in comparison to the non-cavity sample excited at the exciton energy. The results of this target analysis are shown in Figure 3 and Table 1 (also see Figure S3 of the Supporting Information). The species-associated spectra (SAS) for the non-cavity sample closely follow the proposed kinetic model: the initially excited $S_1$* narrows and red shifts into a thermalized state $S_1$, while a CT state emerges, which decays on a much longer time scale. Notably, CT-associated SAS exhibits a consistent spectral peak (1.57 eV) with the absorption of the radical anion determined by electrochemical spectroscopy. In the cavity sample, the spectra are modified by the cavity and generation of polaritons, as mentioned above,[7,33,37] but the overall shapes of the SAS remain consistent with those of the non-cavity sample. Note that we use the same nomenclature for the species $S_1$*, $S_1$, and CT for simplicity, but the $S_1$ (and $S_1$*) named state has a polariton character in the cavity sample. When pumped at the LP, $k_1$ is increased due to reduced thermalization, while $k_2$ is significantly increased, leading to a higher CT yield ($\frac{k_2}{k_2+k_3}$). The rate constant $k_3$ is largely unchanged, indicating a lifetime comparable between that of the LP and exciton. Pumping at the UP results in different $k_1$ and $k_3$, likely due to the complexity of UP decay channels that cannot be fully resolved within this simplified model, i.e., UP relaxation to the LP, and because both uncoupled excitons and LP states are also excited as they are not far separated in energy. Across all excitation conditions, $k_4$ remains largely unchanged, indicating a reliable measurement of the CT state decay. Excitation at the exciton energy yields rate constants intermediate between those of UP and LP excitation, consistent with partial excitation of UP, uncoupled exciton, and LP states, and is within error from the UP and LP excitation. Measurements on the non-cavity sample (Table S2 of the Supporting Information) show a dependence of the thermalization rate ($k_1$) on fluence, while $k_2$, $k_3$, and $k_4$ remain consistent and fluence-independent. This further confirms that the increase in $k_2$ is not simply due to a higher excitation density in the cavity but arises directly from the polariton coupling.

As depicted in Figure 4, $k_2$ in the kinetic model represents the transition from the $S_1$ to CT state in the photophysical

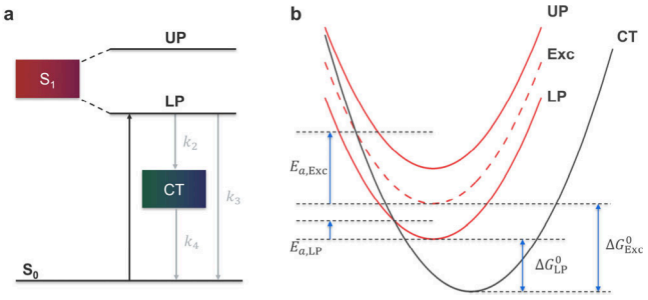


Figure 4. (a) Photophysical state diagram of the cavity sample, with $k_2$ representing LP → CT, which is posited to be in the Marcus inverted regime, reduced due to a lower driving force. (b) Potential energy surfaces of the exciton, UP, LP, and CT states in the Marcus inverted regime. The activation energy and the driving force are both reduced by the formation of LP.

diagram. Reported reorganization energies for bay-substituted PDI molecules typically fall in the range $\lambda \approx 0.26-0.32$ eV.[38,39] While direct measurements of the driving force $\Delta G^0$ are lacking, several studies suggest that the observed CT is intramolecular in nature.[40−42] In such cases, $\Delta G^0$ includes contributions from exciton binding energy and electrostatic stabilization of the separated charges. The exciton binding energy can be estimated from the bandgap $E_b \approx 0.72$ eV,[43] whereas the stabilization energy is more difficult to evaluate without first-principles calculations. Enhanced $k_2$ observed upon LP excitation indicates that $|\Delta G^0|$ exceeds $\lambda$ in this system, placing it within the Marcus inverted regime, where the


https://doi.org/10.1021/acs.jpclett.5c02566
J. Phys. Chem. Lett. 2026, 17, 790−796

CT rate decreases with an increasing driving force. In the cavity system, the formation of the LP effectively reduces the driving force, as suggested by the slight blue shift of the CT-associated spectrum. This reduction in $|\Delta G^0|$ moves the system toward the activationless region of the Marcus curve, leading to the enhanced CT rate and yield observed experimentally. This behavior was predicted theoretically for a similar polariton-coupled charge transfer system,[44] and our results experimentally confirm that light−matter strong coupling can tune the CT within the Marcus inverted regime by modifying the effective driving force through polariton formation.

In summary, we have demonstrated strong light−matter coupling in a DBR microcavity incorporating the bay-substituted PDI derivative b-PDI-1,6,7,12, evidenced by Rabi splitting and polariton dispersion in angle-resolved reflectance. Ultrafast transient absorption spectroscopy under different excitation energies reveals that the system operates within the Marcus inverted regime and that excitation at the LP enhances the formation of CT states. This enhancement is attributed to the reduced driving force resulting from the lower polariton state, placing the system deeper into the Marcus inverted regime. These results suggest that cavity coupling can modulate intramolecular charge transfer by reshaping the electronic potential energy surfaces through light−matter hybridization, which highlights how cavity quantum electrodynamics can be used to modulate excited-state dynamics, offering new strategies for controlling charge separation processes in organic semiconductors.

## ■ ASSOCIATED CONTENT

### Data Availability Statement

The data that support the findings of this study are available within the paper and its Supporting Information. Source data are available from the corresponding author upon reasonable request.

### Supporting Information

The Supporting Information is available free of charge at https://pubs.acs.org/doi/10.1021/acs.jpclett.5c02566.

Experimental methods and additional experimental details, including optical constants of materials, cyclic voltammogram experiment results, and fitting details of the target analysis (PDF)

Transparent Peer Review report available (PDF)

## ■ AUTHOR INFORMATION


### Corresponding Author

**Jao van de Lagemaat** − *Chemistry and Nanoscience Center, National Laboratory of the Rockies, Golden, Colorado 80401, United States; Materials Science and Engineering Program, University of Colorado, Boulder, Colorado 80303, United States; Renewable and Sustainable Energy Institute, National Renewable Energy Laboratory and University of Colorado, Boulder, Colorado 80309, United States;* orcid.org/0000-0001-5851-6163; Email: jao.vandelagemaat@nrel.gov

### Authors

**Rao Fei** − *Chemistry and Nanoscience Center, National Laboratory of the Rockies, Golden, Colorado 80401, United States; Materials Science and Engineering Program, University of Colorado, Boulder, Colorado 80303, United States;* orcid.org/0000-0002-4034-2967

**Victoria Quirós-Cordero** − *School of Materials Science and Engineering, Georgia Institute of Technology, Atlanta, Georgia 30332, United States*

**Demelza Wright** − *Chemistry and Nanoscience Center, National Laboratory of the Rockies, Golden, Colorado 80401, United States;* orcid.org/0000-0002-8854-2714

**Debjit Ghoshal** − *Chemistry and Nanoscience Center, National Laboratory of the Rockies, Golden, Colorado 80401, United States;* Present Address: Indian Institute of Technology Guwahati, Guwahati, Assam 781039, India; orcid.org/0000-0003-3204-0755

**Justin C. Johnson** − *Chemistry and Nanoscience Center, National Laboratory of the Rockies, Golden, Colorado 80401, United States; Renewable and Sustainable Energy Institute, National Renewable Energy Laboratory and University of Colorado, Boulder, Colorado 80309, United States;* orcid.org/0000-0002-8874-6637

**Ivan I. Smalyukh** − *Materials Science and Engineering Program, University of Colorado, Boulder, Colorado 80303, United States; Department of Physics, University of Colorado, Boulder, Colorado 80309, United States; International Institute for Sustainability with Knotted Chiral Meta Matter, Hiroshima University, Higashihiroshima, Hiroshima 739-8526, Japan; Renewable and Sustainable Energy Institute, National Renewable Energy Laboratory and University of Colorado, Boulder, Colorado 80309, United States;* orcid.org/0000-0003-3444-1966

**Carlos Silva-Acuña** − *Institut Courtois, Université de Montréal, Montréal, Québec H2V 0B3, Canada;* orcid.org/0000-0002-3969-5271

**Natalie Stingelin** − *School of Materials Science and Engineering, Georgia Institute of Technology, Atlanta, Georgia 30332, United States;* orcid.org/0000-0002-1414-4545

Complete contact information is available at: https://pubs.acs.org/10.1021/acs.jpclett.5c02566


### Notes

The authors declare no competing financial interest.

## ■ ACKNOWLEDGMENTS

This work was authored by the National Laboratory of the Rockies for the U.S. department of Energy (DOE), operated under Contract No. DE-AC36-08GO28308. Funding provided by the U.S. Department of Energy Office of Science, Office of Basic Energy Sciences, Division of Chemical Sciences, Geosciences, and Biosciences, Photochemistry Program. V.Q.C. and C.S. gratefully acknowledge funding by the by the U.S. National Science Foundation Science and Technology Center (STC) for Integration of Modern Optoelectronic Materials on Demand (IMOD) under Cooperative Agreement No. DMR-2019444. V.Q.C. contributed to this work through cavity design, fabrication, and initial characterization, as well as writing the corresponding sections of this manuscript together with N.S. and C.S. N.S. in addition thanks the European Research Council's support via a Starting Independent Researcher Project under the grant agreement No. 279587, that had provided the important monetary support and scientific freedom to start N.S. to work in an entirely new field. C.S.A. acknowledges funding from the Government of

Canada (Canada Excellence Research Chair CERC-2022-00055) and support from the Institut Courtois, Faculté des arts et des sciences, Université de Montréal (Chaire de recherche du directeur de l'Institut Courtois). The authors acknowledge the experimental support and discussion from all authors. The views expressed in the article do not necessarily represent the views of the DOE or the U.S. Government. The U.S. Government retains and the publisher, by accepting the article for publication, acknowledges that the U.S. Government retains a nonexclusive, paid-up, irrevocable, worldwide license to publish or reproduce the published form of this work, or allow others to do so, for U.S. Government purposes.

## REFERENCES

(1) Törmä, P.; Barnes, W. L. Strong coupling between surface plasmon polaritons and emitters: a review. *Rep. Prog. Phys.* **2015**, *78* (1), 013901.
(2) Ebbesen, T. W. Hybrid light−matter states in a molecular and material science perspective. *Acc. Chem. Res.* **2016**, *49* (11), 2403−2412.
(3) Herrera, F.; Owrutsky, J. Molecular polaritons for controlling chemistry with quantum optics. *J. Chem. Phys.* **2020**, *152* (10), 100902.
(4) Kéna-Cohen, S.; Forrest, S. R. Room-temperature polariton lasing in an organic single-crystal microcavity. *Nat. Photonics* **2010**, *4* (6), 371−375.
(5) Ribeiro, R. F.; et al. Polariton chemistry: controlling molecular dynamics with optical cavities. *Chem. Sci.* **2018**, *9* (30), 6325−6339.
(6) Feist, J.; Garcia-Vidal, F. J. Extraordinary exciton conductance induced by strong coupling. *Phys. Rev. Lett.* **2015**, *114* (19), 196402.
(7) Fei, R.; et al. Controlling exciton/exciton recombination in 2-d perovskite using exciton-polariton coupling. *J. Phys. Chem. Lett.* **2024**, *15* (6), 1748−1754.
(8) Ballarini, D.; et al. Polaritonic neuromorphic computing outperforms linear classifiers. *Nano Lett.* **2020**, *20* (5), 3506−3512.
(9) Gomez-Dominguez, M.; et al. Multiple emission peaks challenge polariton condensation in phenethylammonium-based 2d perovskite microcavities. *ACS Photonics* **2025**, *12* (5), 2423−2431.
(10) Georgiou, K.; Jayaprakash, R.; Othonos, A.; Lidzey, D. G. Ultralong-range polariton-assisted energy transfer in organic microcavities. *Angew. Chem.* **2021**, *133* (30), 16797−16803.
(11) Eizner, E.; Martínez-Martínez, L. A.; Yuen-Zhou, J.; Kéna-Cohen, S. Inverting singlet and triplet excited states using strong light−matter coupling. *Sci. Adv.* **2019**, *5* (12), No. eaax4482.
(12) Polak, D.; et al. Manipulating molecules with strong coupling: harvesting triplet excitons in organic exciton microcavities. *Chem. Sci.* **2020**, *11* (2), 343−354.
(13) Lee, I.; Melton, S. R.; Xu, D.; Delor, M. Controlling molecular photoisomerization in photonic cavities through polariton funneling. *J. Am. Chem. Soc.* **2024**, *146* (14), 9544−9553.
(14) Wu, W.; Sifain, A. E.; Delpo, C. A.; Scholes, G. D. Polariton enhanced free charge carrier generation in donor−acceptor cavity systems by a second-hybridization mechanism. *J. Chem. Phys.* **2022**, *157* (16), 161102.
(15) Borges, L.; Schnappinger, T.; Kowalewski, M. Impact of dark polariton states on collective strong light−matter coupling in molecules. *J. Phys. Chem. Lett.* **2025**, *16*, 7807−7815.
(16) Bhuyan, R.; Lednev, M.; Feist, J.; Börjesson, K. The effect of the relative size of the exciton reservoir on polariton photophysics. *Adv. Opt. Mater.* **2024**, *12* (2), 2301383.
(17) Pandya, R.; et al. Tuning the coherent propagation of organic exciton-polaritons through dark state delocalization. *Adv. Sci.* **2022**, *9* (18), 2105569.
(18) Groenhof, G.; Climent, C.; Feist, J.; Morozov, D.; Toppari, J. J. Tracking polariton relaxation with multiscale molecular dynamics simulations. *J. Phys. Chem. Lett.* **2019**, *10* (18), 5476−5483.
(19) Koessler, E. R.; Mandal, A.; Musser, A. J.; Krauss, T. D.; Huo, P. Polariton mediated electron transfer under the collective molecule-cavity coupling regime. *Chem. Sci.* **2025**, *16*, 11644−11658.
(20) Würthner, F. Perylene bisimide dyes as versatile building blocks for functional supramolecular architectures. *Chem. Commun.* **2004**, *14*, 1564−1579.
(21) Chen, Z.; Lohr, A.; Saha-Möller, C. R.; Würthner, F. Self-assembled pi-stacks of functional dyes in solution: structural and thermodynamic features. *Chem. Soc. Rev.* **2009**, *38* (2), 564−584.
(22) Langhals, H. Control of the stacking of perylene bisimide dyes in solution by introduction of bulky substituents. *Helv. Chim. Acta* **2005**, *88* (6), 1309−1343.
(23) Sung, J.; et al. Direct observation of excimer-mediated intramolecular electron transfer in a cofacially-stacked perylene bisimide pair. *J. Am. Chem. Soc.* **2016**, *138* (29), 9029−9032.
(24) Royakkers, J.; et al. Doubly encapsulated perylene diimides: effect of molecular encapsulation on photophysical properties. *J. Org. Chem.* **2020**, *85* (1), 207−214.
(25) Hestand, N. J.; Spano, F. C. Interference between coulombic and CT-mediated couplings in molecular aggregates: H- to J-aggregate transformation in perylene-based π-stacks. *J. Chem. Phys.* **2015**, *143* (24), 244707.
(26) Strang, A.; et al. Simple and versatile platforms for manipulating light with matter: strong light−matter coupling in fully solution-processed optical microcavities. *Adv. Mater.* **2024**, *36* (20), 2212056.
(27) McGhee, K. E.; et al. Polariton condensation in an organic microcavity utilising a hybrid metal-DBR mirror. *Sci. Rep.* **2021**, *11* (1), 20879.
(28) Liu, B.; Rai, P.; Grezmak, J.; Twieg, R. J.; Singer, K. D. Coupling of exciton-polaritons in low-Q coupled microcavities beyond the rotating wave approximation. *Phys. Rev. B* **2015**, *92* (15), 155301.
(29) Russo, M.; et al. One-pot synthesis of polymer/inorganic hybrids: toward readily accessible, low-loss, and highly tunable refractive index materials and patterns. *J. Polym. Sci., Part B: Polym. Phys.* **2012**, *50* (1), 65−74.
(30) Bachevillier, S.; et al. Fully solution-processed photonic structures from inorganic/organic molecular hybrid materials and commodity polymers. *Adv. Funct. Mater.* **2019**, *29* (21), 1808152.
(31) Bachevillier, S.; et al. Planar refractive index patterning through microcontact photo-thermal annealing of a printable organic/inorganic hybrid material. *Mater. Horiz.* **2022**, *9* (1), 411−416.
(32) Kang, S.; et al. Ultrafast coherent exciton dynamics in size-controlled perylene bisimide aggregates. *Struct. Dyn.* **2019**, *6* (6), 064501.
(33) Schwennicke, K.; et al. When do molecular polaritons behave like optical filters? *Chem. Soc. Rev.* **2025**, *54* (13), 6482.
(34) Deng, S.; Yang, J.; Shao, Y.; Ou, Q.; Shuai, Z. Optical emission spectra of molecular excitonic polariton computed at the first-principles level QED-TDDFT. *ChemPhotoChem* **2024**, *8* (12), No. e202400117.
(35) Kaufmann, C.; et al. Ultrafast exciton delocalization, localization, and excimer formation dynamics in a highly defined perylene bisimide quadruple π-stack. *J. Am. Chem. Soc.* **2018**, *140* (12), 4253−4258.
(36) Sung, J.; Kim, P.; Fimmel, B.; Würthner, F.; Kim, D. Direct observation of ultrafast coherent exciton dynamics in helical π-stacks of self-assembled perylene bisimides. *Nat. Commun.* **2015**, *6* (1), 8646.
(37) Yasukuni, R.; et al. Modification of excimer emission of perylene dye thin films by single silver nanocubes. *J. Photochem. Photobiol. A: Chem.* **2011**, *221* (2−3), 194−198.
(38) Idé, J.; et al. Supramolecular organization and charge transport properties of self-assembled π- π stacks of perylene diimide dyes. *J. Phys. Chem. B* **2011**, *115* (18), 5593−5603.
(39) Ruiz Delgado, M. C.; Kim, E. G.; da Silva Filho, D. A.; Bredas, J. L. Tuning the charge-transport parameters of perylene diimide single crystals via end and/or core functionalization: a density


https://doi.org/10.1021/acs.jpclett.5c02566
J. Phys. Chem. Lett. 2026, 17, 790−796

functional theory investigation. *J. Am. Chem. Soc.* **2010**, *132* (10), 3375−3387.
(40) Kang, S.; et al. Impact of packing geometry on excimer characteristics and mobility in perylene bisimide polycrystalline films. *ACS Appl. Mater. Interfaces* **2024**, *16* (14), 18134−18143.
(41) Inan, D.; et al. Substitution effects on the photoinduced charge-transfer properties of novel perylene-3, 4, 9, 10-tetracarboxylic acid derivatives. *J. Phys. Chem. A* **2017**, *121* (24), 4633−4644.
(42) Edvinsson, T.; et al. Intramolecular charge-transfer tuning of perylenes: spectroscopic features and performance in dye-sensitized solar cells. *J. Phys. Chem. C* **2007**, *111* (42), 15137−15140.
(43) Sugie, A.; Nakano, K.; Tajima, K.; Osaka, I.; Yoshida, H. Dependence of exciton binding energy on bandgap of organic semiconductors. *J. Phys. Chem. Lett.* **2023**, *14* (50), 11412−11420.
(44) Mandal, A.; Krauss, T. D.; Huo, P. Polariton-mediated electron transfer via cavity quantum electrodynamics. *J. Phys. Chem. B* **2020**, *124* (29), 6321−6340.



https://doi.org/10.1021/acs.jpclett.5c02566
*J. Phys. Chem. Lett.* 2026, 17, 790−796